Functional anatomy of neural circuits regulating fear and extinction

Ewelina Knapska[a,1], Matylda Macias[b,c], Marta Mikosz[a], Aleksandra Nowak[a], Dorota Owczarek[b], Marcin Wawrzyniak[b], Marcelina Pieprzyk[c], Iwona A. Cymerman[c], Tomasz Werka[a], Morgan Sheng[d,2], Stephen Maren[e], Jacek Jaworski[c,1], and Leszek Kaczmarek[b,1]

Departments of [a]Neurophysiology and [b]Molecular and Cellular Neurobiology, Nencki Institute of Experimental Biology, 02-093 Warsaw, Poland; [c]International Institute of Molecular and Cell Biology, 02-109 Warsaw, Poland; [d]Picower Institute for Learning and Memory, Massachusetts Institute of Technology, Cambridge, MA 02139; and [e]Department of Psychology and Institute for Neuroscience, Texas A&M University, College Station, TX 77843-3474

The memory of fear extinction is context dependent: fear that is suppressed in one context readily renews in another. Understanding of the underlying neuronal circuits is, therefore, of considerable clinical relevance for anxiety disorders. Prefrontal cortical and hippocampal inputs to the amygdala have recently been shown to regulate the retrieval of fear memories, but the cellular organization of these projections remains unclear. By using anterograde tracing in a transgenic rat in which neurons express a dendritically-targeted PSD-95:Venus fusion protein under the control of a c-*fos* promoter, we found that, during the retrieval of extinction memory, the dominant input to active neurons in the lateral amygdala was from the infralimbic cortex, whereas the retrieval of fear memory was associated with greater hippocampal and prelimbic inputs. This pattern of retrieval-related afferent input was absent in the central nucleus of the amygdala. Our data show functional anatomy of neural circuits regulating fear and extinction, providing a framework for therapeutic manipulations of these circuits.

gene expression | hippocampus | prefrontal cortex | learning and memory

There is an increasing interest in the neural mechanisms underlying extinction of learned fear, in part because fear extinction is a useful model for exposure-based therapies for the treatment of human anxiety disorders, such as phobias and posttraumatic stress disorder (1). During fear extinction, a previously conditioned stimulus (CS) is repeatedly presented in the absence of the unconditioned stimulus (US), a procedure that induces a progressive decrease in the magnitude and probability of learned fear responses, including freezing behavior. However, extinction does not erase the original fear memory; rather, it promotes the formation of a new inhibitory memory that reduces fear to the CS (2). Extinguished fear is highly context dependent, insofar as CS presentation outside the extinction context results in the recovery of the previously conditioned fear response, a phenomenon known as fear renewal (3). The return of fear after extinction is a considerable challenge for the efficacy of exposure-based therapies (4). Therefore, identification of brain structures and neuronal circuits selectively implicated in extinction vs. renewal of fear is of great importance.

Owing to substantial progress toward understanding the neural mechanisms underlying the context specificity of fear extinction, there is now a general consensus that, for auditory fear conditioning, extinction involves three main structures: the amygdala, hippocampus (HIPP), and prefrontal cortex (PFC) (2, 5–8). However, the neuronal interactions between these structures that underlie contextual retrieval of fear memory after extinction remain to be elucidated. This problem is further complicated by the fact that neither the amygdala nor the PFC is a homogeneous structure. Among the substructures of the amygdala, the central, basal, and lateral nuclei (Ce, Ba, and La, respectively) have been implicated in the contextual regulation of extinction memories (2). There is also growing evidence for subregional differences within the PFC: the infralimbic (IL) and prelimbic (PL) cortices have opposite influences on fear expression, inhibiting and exciting amygdala output, respectively (9–11). Moreover, convergent inputs

from both the PL and ventral HIPP (vHIPP) in the Ba mediate fear renewal (12). Recently, Herry et al. (13) have shown that rapid transitions between behavioral states of low and high fear, evoked by fear extinction and its context-dependent renewal, respectively, can be triggered by a switch in the balance of activity between two distinct populations of Ba neurons, which appear to be integrated into discrete neuronal circuits differentially connected with the HIPP and PFC. It remains unknown whether similarly functional neurons exist also in Ce and La amygdala subdivisions. Furthermore, the synaptic organization of HIPP and PFC inputs to the amygdala that might underlie functional switches in fear output is not known, especially as far as differential function of IL vs. PL is concerned.

To address the aforementioned questions, we used newly generated transgenic rats expressing a PSD-95:Venus fusion protein under the control of a c-*fos* promoter and targeted to dendrites using the PSD-95 and 3′-UTR of *Arc* mRNA. Before behavioral testing, these rats were injected with anterograde tracers into the vHIPP as well as PL and IL subdivisions of the medial prefrontal cortex. This functional tract tracing procedure allowed us to examine the pattern of hippocampal and prefrontal cortical input onto the cell bodies and dendrites of behaviorally active neurons in the amygdala.

Results

We first generated a tool ("Venus rat") to visualize synapses of activated neurons. Because PSD-95 is a major component of postsynaptic densities, *Arc* UTR contains dendrite localizing sequences, and c-*fos* promoter is induced by neuronal activity, Venus rats allow the dendrites and synapses of activated neurons to be visualized with fluorescent tags (Fig. 1A). In our Venus rat, we have placed reporter protein under the control of a shortened c-*fos* sequence that encodes only the first four amino acids of c-Fos and therefore lacks the nuclear localization signal. Such an approach preserves promoter inducibility, allowing at the same time visualization of neuronal morphology (14).

As a proof of concept for our strategy, we cultured neurons from transgenic rats and analyzed the expression, inducibility, and cellular distribution of PSD95:Venus. As shown in Fig. 1 B and C, PSD-95:Venus could not be detected in cortical or hippocampal neurons cultured under basal conditions. However, application of 50 μM bicuculline, which increases neuronal activity by suppressing
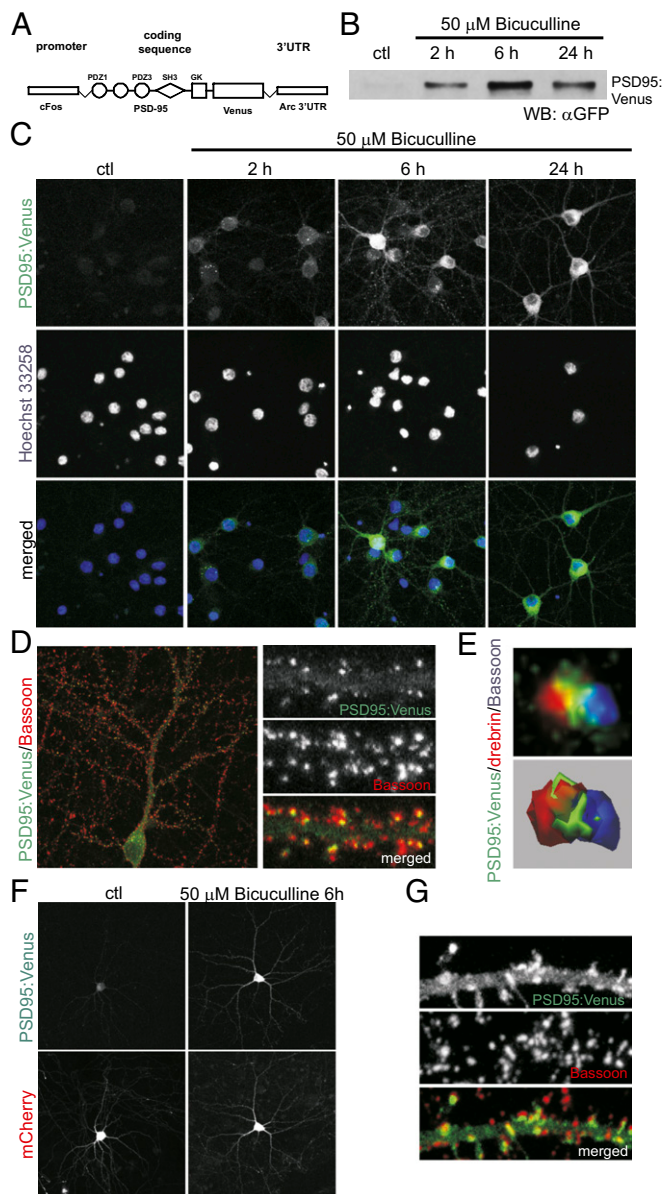
NEUROSCIENCE

Fig. 1. c-Fos-PSD95:Venus-Arc transgene is induced by neuronal activity and expresses a marker of the synaptodendritic compartment in cultured neurons. (*A*) Schematic representation of a c-Fos-PSD-95:Venus-Arc transgenization cassette. (*B*) Western blot analysis of PSD-95:Venus expression in transgenic cortical neurons cultured in vitro under basal conditions and after increased neuronal network activity (50 µM bicuculline treatment). (*C*) Immunofluorescence analysis of PSD-95:Venus expression in transgenic hippocampal neurons cultured in vitro under basal conditions and after increased neuronal network activity (50 µM bicuculline treatment). (*D*) Representative image of double-immunofluorescent labeling of transgenic neuron (6 h post bicuculline) for Venus (with anti-GFP antibody) and the presynaptic marker, Bassoon, showing localization of PSD-95:Venus to synapses. (*E*) Three-dimensional reconstruction of a single synapse of a transgenic neuron immunofluorescently stained for Venus, Bassoon, and the postsynaptic protein, drebrin. (*Upper*) Raw image. (*Lower*) Three-dimensional reconstruction. (*F*) Analysis of PSD-95:Venus expression, transfected to wild-type DIV14 amygdalar neurons cultured in vitro, 4 d posttransfection under basal conditions and 6 h after increased neuronal network activity (50 µM bicuculline treatment). Cells were cotransfected with plasmid encoding mCherry for identification of transfected neurons. (*G*) Representative image of double-immunofluorescent labeling of amygdalar neuron (6 h post bicuculline), transfected as in *F*, for Venus (with anti-GFP antibody) and the presynaptic marker, Bassoon, showing localization of PSD-95:Venus to synapses.

inhibitory transmission, resulted in robust induction of transgene-encoded protein at all tested time points. PSD-95:Venus puncta were observed at 6 and 24 h (Fig. 1*C*), suggesting its incorporation into postsynaptic sites. This was further confirmed by double- and triple-immunofluorescence (IF) staining for Venus (with use of anti-GFP antibody), Bassoon (presynaptic marker; Fig. 1*D*), and drebrin (postsynaptic marker; Fig. 1*E*). Three-dimensional reconstruction of confocal images of individual spine confirmed presence of PSD-95:Venus at the conjunction of presynaptic and postsynaptic sites. Similar results have been obtained when the plasmid used for generation of transgenic animals was transfected into amygdalar neurons of wild-type rats cultured in vitro (Fig. 1 *F* and *G*), suggesting that the construct we designed behaves as predicted also in the amygdala neurons.

Once we confirmed our transgenic model in cultured cells, we examined whether fear conditioning induces transgene expression and drives transgenic protein into synaptodendritic compartment in the behaving animals. Venus rats were subjected to fear conditioning and killed 2, 6, 24, or 72 h after training. As shown in Fig. 2*A*, in the lateral amygdala we observed expression of PSD95:Venus as soon as 2 h after fear conditioning. In the control conditions (exposure to the experimental cage), the transgene expression was much lower. Importantly, strong expression of the transgene was observed in cells stained for endogenous c-Fos, further validating our experimental animal model (Fig. 2*B*). On the other hand, expression of PSD95:Venus persisted up to 24 h after training, which is much longer than expression of endogenous c-Fos; this allowed us to track the history of individual neurons' activation. To trace convergent input at the dendrites and synapses of such neurons, we performed double-IF staining for Venus/MAP2 and Venus/synaptophysin 24 h after fear conditioning. As shown in Fig. 2*C*, PSD-95:Venus was localized to the dendrites and its punctuate staining coincided with IF of presynaptic synaptophysin. Thus, we conclude that the Venus rat is an appropriate animal model for reporting dendritic loci of neuronal activity.

We next explored the pattern of hippocampal (HIPP) and prefrontal cortical (IL and PL) convergence in the amygdala (La and Ce) after the retrieval of fear and extinction memories. Rats were injected with anterograde axonal transport tracers [tetramethylrhodamine (FluoroRuby; FR) and *Phaseolus vulgaris*-leucoagglutinin (PHA-L)] in the IL, PL, or vHIPP. Only rats with FR or PHA-L labeling confined to the IL, PL, or vHIPP were included in the analyses (Fig. S1). The infusions into the vHIPP covered a relatively large part of the structure; however, it has been shown that direct projections to the La and Ce originate primarily in the most ventral part of the CA1 and subiculum (15).

After recovery, the Venus rats were subjected to fear conditioning, extinction, and retrieval testing; the behavioral performance of the rats was typical and rats exhibited robust context-dependent retrieval of fear memory (Fig. S2). Rats tested outside the extinction context (HIGH FEAR) exhibited renewal of fear response to the extinguished CS, whereas the rats tested within the extinction context (LOW FEAR) displayed low levels of fear (Fig. 3*A*). Activated neurons, as visualized by Venus protein expression, were located throughout the amygdala, in all of its major subdivisions, including the lateral and central nuclei. To quantify the nature and degree of convergence of either hippocampal or cortical input onto the target neurons, we computed ratios of the number of fibers for each anterograde tracer impinging onto individual neurons. The ratios of vHIPP/PFC and IL/PL projections were calculated for activated (Venus-positive) neurons within the La and Ce (Fig. 3 *B* and *C*, Table S1). In the La, there was a significant difference between the HIGH FEAR and LOW FEAR groups for the ratio of both vHIPP/PFC projections and IL/PL projections. Specifically, the ratio of vHIPP/PFC projections was greater in rats renewing their fear outside the extinction context relative to rats tested in the extinction context. Within the PFC, the ratio of IL/PRL projections was greatest in rats expressing extinction. These results reveal that neurons in the La that are active during the renewal of fear receive proportionately

greater input from the vHIPP and PRL, whereas La neurons that are active during the suppression of fear during extinction receive proportionally greater input from the IL. In a striking contrast, such differences were not observed in the Ce.

Retrieval testing in our behavioral paradigm was performed 5 d after the extinction session to allow for the decay of PSD95: Venus transgene expression after fear conditioning (the transgene decays to the basal level after 72 h). To exclude the possibility that the extinction session that followed fear conditioning also elevated PSD95:Venus expression (and summated with retrieval-induced transgene expression), we examined the level of transgene expression in rats 5 d after extinction without retrieval testing (HC group). We found that the level of PSD95:Venus expression was very low and apparently significantly lower than both fear-conditioned rats (FC group) as well as the LOW FEAR and HIGH FEAR groups (Table S2). Moreover, we quantified colocalization of PSD-95:Venus construct and endogenous c-Fos in the amygdala following fear conditioning and extinction memory retrieval in the LOW FEAR and HIGH FEAR groups. We found that most of the PSD-95:Venus-positive neurons were also stained for endogenous c-Fos (Table S3).

To further characterize the pattern of hippocampal and prefrontal cortical innervation of La neurons in the two retrieval conditions, we performed a more detailed analysis that focused on the proportion of La neurons in individual rats that showed differential innervation (Fig. 3D). For this analysis, the percentage of neurons in each rat with different ratios of vHIPP/ PFC and IL/PL projections was counted. Most of the active cells in rats from the HIGH FEAR group (71%) were more densely

innervated by the vHIPP than by the PFC. This ratio was opposite for rats in the LOW FEAR group, in which 66% of cells received more inputs from the PFC than from the vHIPP. Moreover, the majority of active La neurons in the LOW FEAR group received greater inputs from the IL (85%), whereas 66% of La neurons in the HIGH FEAR group received projections primarily from the PL (Fig. 4).

The group specificity of the observed differences is further supported by the ratio of overall projections from the vHIPP/ PFC and IL/PL to the La, which was very similar for both the LOW FEAR and HIGH FEAR groups (vHIPP/PFC: LOW FEAR, 2.36 ± 0.79; HIGH FEAR, 2.39 ± 0.87; IL/PL: LOW FEAR, 1.84 ± 0.07; HIGH FEAR, 1.90 ± 0.24). The overall projections ratios were calculated for the whole images, including both active and inactive neurons.

Hence, our data reveal two subpopulations of neurons within the La that have preferential connections either to the IL or PL and vHIPP; the former are more active during retrieval of fear extinction memory, whereas the latter are more active during retrieval of the fear memory. This suggests that neuronal populations within the La that are activated by fear extinction and renewal are, at least partially, different. To examine this idea further, we analyzed the number of Venus-positive cells observed in the La in rats given a single retention test (either inside or outside the extinction context) and in rats given retention tests in both contexts (a within-subject test of context-dependent memory retrieval). Indeed, we observed a greater number of activated neurons within the La in rats tested in both contexts in comparison with rats tested in a single context (single test: 75 ± 13, $n = 4$; double test: 136 ± 17, $n = 8$; $P < 0.05$).

Discussion

In aggregate, the present data reveal two distinct subpopulations of neurons within the La that are activated by the retrieval of extinction memory and the context-dependent renewal of conditioned fear. They can be distinguished by their connections to the vHIPP and the IL and PL divisions of the PFC. The neuronal circuit in the La whose activity is correlated with elevated freezing during fear renewal is preferentially innervated by the vHIPP and PL, whereas the neurons whose activity is correlated with low freezing during the suppression of fear in the extinction context receive input mainly from the IL. In contrast, no such differences were observed in the Ce.

These results were obtained with an experimental model that we have developed, namely the c-Fos-PSD-95:Venus-Arc transgenic rat, in which expression of a transgene was narrowed to a population of active cells and PSD-95:Venus localized to synaptodendritic compartment (Figs. 1 and 2). mRNA and proteins encoded by immediate early genes such as c-Fos, Arc, or Homer are widely used as markers of neuronal activation in behavioral studies including studies on fear (16). However, they only allow one to study a cohort of active cells for a few hours after neuronal activation. Thus, several groups have developed reporter mice based on c-fos promoter sequences driving expression of enzymes (β-gal) (17) or fluorescent proteins (GFP) (18) that can be easily detected and are more stable, but in most cases do not specifically highlight synapses. Recently, another model for visualizing synapses has been developed. GFP-GluR1c-fos Tg mice have been generated and used to study learning-associated recruitment of newly synthesized GFP-tagged GluA subunit of AMPA-type glutamate receptors to spines (19). In this case, the GluA coding sequence was placed under control of tetracycline responsive element and the c-fos promoter was used to control expression of the tetracycline transactivator. This type of system, although it tightens control of transgene expression, requires, however, additional drug treatments. Because leakiness was not an issue in our Venus rat model (Fig. 2), setup simplicity is an advantage of our experimental model. Finally, in contrast to all of the above models, we generated a transgenic rat instead of the more typical mouse models. This is advantageous in several ways,
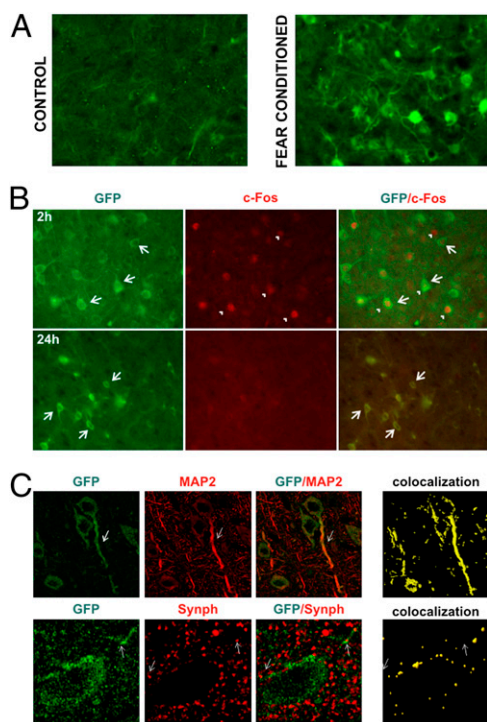

Fig. 2. Characterization of c-Fos-PSD95:Venus-Arc transgenic rats. (A) Expression of the fusion PSD-95:Venus protein (Venus-positive, green) was visible in the lateral amygdala 2 h after fear conditioning training, whereas its expression was much lower in control (nonshocked) animals. (B) The cells that expressed PSD-95:Venus protein were also positive for endogenous c-Fos (red). The PSD-95:Venus signal was still visible 24 h after fear conditioning, when endogenous c-Fos staining was already absent. $n = 2$–3 per time point. (C) Double immunostaining for Venus/MAP2 (dendritic marker) and Venus/synaptophysin (presynaptic marker) 24 h after fear conditioning. PSD-95:Venus was localized to dendrites and its punctate staining partly overlapped with the presynaptic marker.

Fig. 3. The proportion of afferent projections from vHIPP and PFC, as well as the IL and PL cortices on active neurons (Venus-positive) in the ventral part of La and in the lateral part of Ce. (*A*) Two groups of rats were compared: rats tested within the extinction context (LOW FEAR), which showed low level of freezing, and rats tested outside the extinction context (HIGH FEAR), which exhibited renewal of fear to the extinguished CS. (*B*) An example of an active neuron (GFP, green) with afferent anterograde axonal transport tracers labeling the cell (FR, red; PHA-L, magenta). (*C*) Proportion of projections from the vHIPP and PFC or the IL and PL in the La and Ce for the LOW FEAR and HIGH FEAR groups. Most of the cells activated in the La by the renewal of fear received projections from the vHIPP and PL (HIGH FEAR group), whereas neurons activated by the retrieval of extinction memory (LOW FEAR group) received inputs from the PFC, especially from the IL. Such differences were absent in the Ce. The number of animals

used in the study was as follows: for vHIPP/PFC projections, LOW FEAR group, n = 5; HIGH FEAR GROUP, n = 6; for IL/PL projections, LOW FEAR group, n = 5; HIGH FEAR GROUP, n = 5. (*D*) Percentage of neurons with different ratios of vHIPP/PFC and IL/PL projections plotted for each individual rat (the animals numbers correspond with the injection sites numbers showed in Fig. S2); Kolmogorov–Smirnov two-sample test, LOW FEAR vs. HIGH FEAR groups in the cumulative distributions of both vHIPP/PFC and IL/PL projections ratios; **P < 0.01. Error bars indicate mean ± SEM.
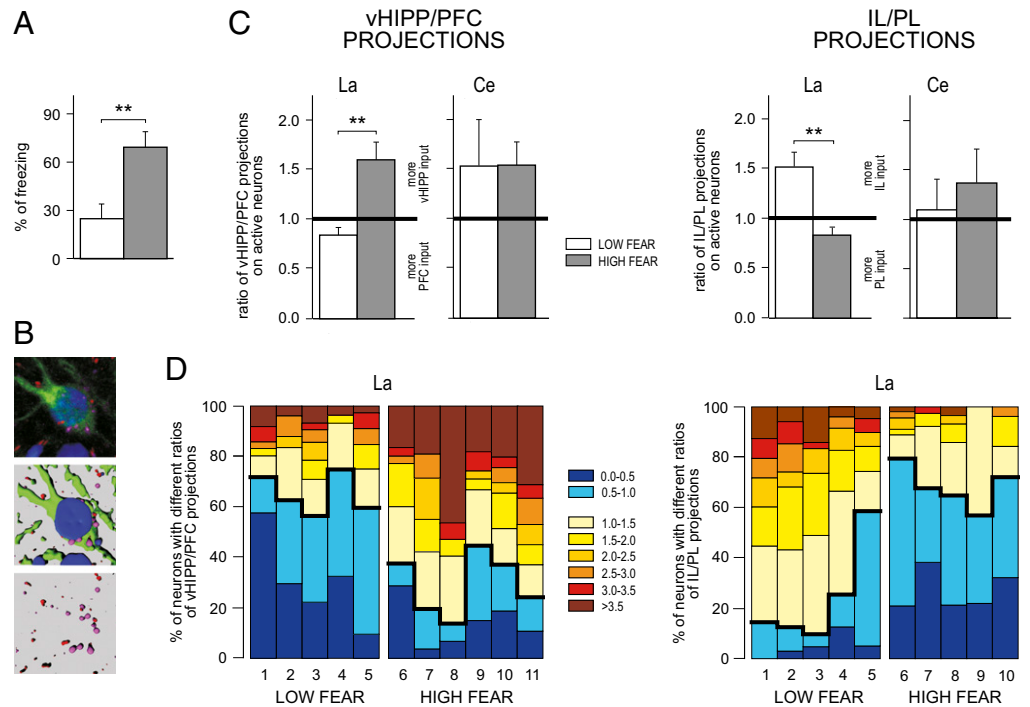
particularly because the rat has been more extensively characterized behaviorally.

The present results elucidate the synaptic organization of HIPP and PFC inputs to the amygdala that might underlie functional switches in fear output. The data support the view that the IL and PL have opposite roles in fear expression (9, 11, 20, 21), as well as an important role for the HIPP in the renewal of extinguished fear (22–27). Furthermore, we show that vHIPP and PL inputs to the La selectively target neurons activated by renewal of fear over neurons activated by retrieval of extinction memory. Thus, both vHIPP and PL inputs to the La neurons may promote fear expression over retrieval of extinction memory. Because the vHIPP is the primary source of contextual information to the amygdala (15) and can influence La activity indirectly via its projections to the PL (28), it is conceivable that the vHIPP contributes to the context dependence of extinction through both direct and indirect projections to the La. Indeed, it has recently been shown that BA-projecting neurons in both the PL and HIPP are preferentially active during the renewal of fear to an extinguished CS and that disconnection of either the direct or indirect routes by which the HIPP projects to the BA impaired the renewal of fear memories after extinction (12).

We have previously shown that both retrieval of extinction memory as well as context-driven renewal of fear result in an increased c-Fos expression in the lateral part of Ce (CeI), whereas the medial part (Cem) is specifically activated by fear renewal (21). Because the CeI receives inputs from the vHIPP, PL, and IL, it is conceivable that context-dependent expression of fear is mediated by the Ce. However, we failed to find specific neuronal circuits differentially connected to the vHIPP, PL, and IL in the Ce. The lack of such circuits is consistent with the view that the Cem inhibition/disinhibition, which plays a role in conditioned fear expression, is mediated by indirect projections from the La to the Cem through the basal amygdala and/or intercalated cells.

Because context-dependent relapse of extinguished fear behavior in humans poses a considerable challenge for the efficacy of exposure-based therapies, identifying the neural networks in-

volved in regulating of fear memory after extinction is essential for the development of more effective therapeutic interventions. Our data suggest an appealing possibility of increasing fear extinction and preventing fear renewal by very specific manipulations of the neurons in the La. In addition, our animal experimental model allows for fluorescence-based identification of individual neurons belonging to specific high-fear vs. low-fear neuronal circuits. This property may be used in further studies for search of specific markers of those cells and their differential identification and thus molecular understanding of their functional specificity. Such an analysis has not been possible until now for the rat, which is a very important experimental model in neurobiology. More generally, the Venus rats may serve as a very useful tool in similar analyses of active circuits engaged in a variety of brain neuronal responses.

Methods

Subjects. Subjects were male PSD-95:Venus transgenic rats (300–400 g at the beginning of the experiment) bred in the Nencki Institute Animal House.
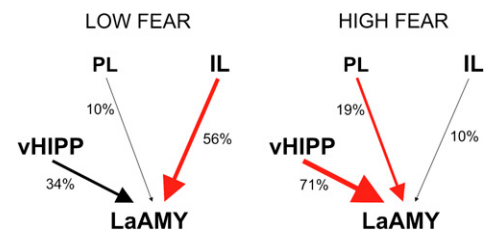
Fig. 4. Percentage of neurons activated by retrieval of the extinction memory (LOW FEAR group) or by renewal of fear (HIGH FEAR group) that received their dominant input from either the vHIPP, PL cortex, and IL cortex. The results suggest that retrieval of extinction memory and renewal of fear activate different subpopulations of neurons within the La, which can be distinguished by their connections to the IL, PL, and vHIPP.

Rats were individually housed in clear plastic cages hanging from a standard stainless-steel rack. All animals were kept under a 12:12-h light–dark cycle, with food and water provided ad libitum. Rats were handled 60 s/d for 4 d before the start of the experiment to habituate them to the experimenter. All experimental procedures were performed in accordance with the Polish Act on Animal Welfare, after obtaining specific permission from the first Warsaw Ethical Committee on Animal Research.

Generation of c-Fos-PSD95Venus-Arc Rats/Genotyping. To generate c-Fos-PSD95:Venus-Arc rats, we first cloned the PSD95 coding sequence from PSD95:GFP plasmid (29) into pEGFP-N1 (CMV-PSD95:GFP-SV40). The *c-fos* promoter fragment (−602 to +1064 with respect to start of transcription) was amplified by PCR from a previously described plasmid used to generate *fos*-LacZ transgenic mice (a kind gift from T. Curran University of Pennsylvania, Philadelphia) (17) and used to replace the CMV promoter sequence with CMV-PSD95:GFP-SV40 (c-Fos-PSD95:GFP-SV40). Next, EGFP1 was exchange into Venus coding sequence (c-Fos-PSD95:Venus-SV40). *Arc* 3′-UTR was PCR-amplified from a plasmid used previously for generation of *Arc*-GFP knock-in mice (a kind gift from K. H. Wang and S. Tonegawa, Massachusetts Institute of Technology, Cambridge, MA) (30) and used to replace SV40 3′ UTR with c-Fos-PSD95:Venus-SV40 (c-Fos-PSD95Venus-Arc). Finally, we used the QuikChange Site-Directed Mutagenesis kit (Stratagene) to introduce PacI restriction sites in front of and behind the c-Fos-PSD95:Venus-Arc trans-genization cassette. Next, PacI-c-Fos-PSD95:Venus-Arc-PacI fragment was used to prepare transgenic rats as described previously (31). Genomic DNA was extracted from the offspring by tail biopsy and founders were identified by PCR with two independent pairs of primers. The primer sequences for the PCR were as follows: 5′-ACGTAAACGGCCACAAGTTC-3′ and 5′-AAGTCGTGC-TGCTTCATGTG-3′ (pair 1); 5′-CGGCCACAAGTTCAGCGTGTC-3′ and 5′-GGCGGC-GGTCACGAACTCCA-3′ (pair 2).

Surgical Procedures. Six or seven days before behavioral training, rats received intracranial injections of anterograde axonal transport tracers tetramethylrhodamine (FR) and PHA-L Alexa Fluor 647 conjugate (Invitrogen; Molecular Probes) into the PFC and vHIPP or the PL and IL divisions of the PFC. One group of rats received unilateral injections into the PFC and vHIPP of the same hemisphere; another group was injected into the PL in one hemisphere and the IL in another hemisphere. The sides of the injection and/or the type of the tracer were counterbalanced between the brain structures.

All surgical instruments were sterilized before surgery. Rats were anesthetized with ketamine (100 mg/kg; i.p.) and xylazine (10 mg/kg; i.m.). Ocular lubricant was used to moisten the eyes and the scalp was shaved. After being placed into the stereotaxic apparatus (David Kopf Instruments), the scalp was disinfected with 70% (vol/vol) alcohol, incised, and retracted. Two small burr holes were drilled to allow for a glass capillary (1.0-mm o.d., 0.5-mm i.d., 50- to 60-μm tip diameter with a silver wire inside; Stoelting) or Hamilton syringe needle (1 μL) to be lowered into the desired part of the brain. The coordinates used were as follows: PFC [anteroposterior (AP), +3.2; mediolateral (ML), ±0.6; dorsoventral (DV), −5.4 and −4.0], vHIPP (AP, −5.3; ML, ±5.5; DV, −7.0), PL (AP, +3.2; ML, ±0.6; DV, −4.0 and −3.7) and IL (AP, + 3.2; ML, ±0.6; DV, −5.4 and −5.1). FR [10% (wt/vol) solution in distilled water] and PHA-L [2.5% (wt/vol) solution in 0.1 M sodium PBS, pH 7.4] were delivered into the PFC, PL, and IL iontophoretically (Midgard Precision Current Source; Stoelting). Cathodal current (5 μA) was delivered (7 s pulses every 7 s) over a 20-min period and the glass capillary remained in place for another 5 min to allow for the diffusion of the tracer. Infusions into the hippocampus were made by pressure injection with a Hamilton syringe (MicroSyringe Pump; World Precision Instruments; 0.5 μL total volume; 25 nL/min for 20 min; the needle remained in place for another 10 min to allow for the diffusion of the tracer). After the injection, the incision was sutured and treated with antibiotic ointment, and the animals were administered an analgesic (Tolfedine; 4 mg/kg; s.c.). To avoid dehydration the animals were given 1 mL of warm 0.95% NaCl/100 g of body weight by s.c. injection. The rats were kept on a heating pad until they recovered from anesthesia before returning to their home cages. The animals were allowed 6–7 d for postoperative recovery.

Behavioral Apparatus. Four identical observation chambers (30.0 × 24.0 × 21.0 cm; Near Infrared Video Fear Conditioning System; Med Associates) were used for all phases of the experiment. The chambers were constructed from aluminum (two side walls) and Plexiglas (rear wall, ceiling, and hinged front door) and were situated in a sound-attenuating chest located in an isolated room. The floor of the chamber consisted of stainless-steel rods wired to a shock source and solid-state grid scrambler (Med Associates) for delivery of footshock (US). Stainless-steel pans were placed underneath the grid floor

before the animals were placed inside the box. House lights within the chambers and lights within the room provided illumination. A speaker mounted outside of a grating in one wall of the chamber was used for the delivery of the acoustic CS. Sensory stimuli were adjusted within these chambers to generate two distinct contexts (A and B). For context A, a house light mounted in the ceiling of the cage was illuminated, and the room lights remained on. The chambers were cleaned with a 1% ammonium hydroxide solution, and stainless-steel pans containing a thin film of the same solution were placed underneath the grid floors before the rats were placed inside to provide a distinct odor. Ventilation fans in each chest supplied background noise (65 dB). Rats were transported to this context in transparent plastic cages. For context B, all room and chamber house lights were turned off; a 60 W red light provided illumination, and the ventilation fans were turned off. White Plexiglas floors were placed on the grid of each chamber, and chambers were cleaned with a 1% acetic acid solution. Additionally, stainless-steel pans containing a thin film of this solution were placed underneath the floors before the rats were placed inside. Rats were transported to this context in black plastic boxes with bedding. Freezing behavior was recorded by a camera above each chamber and video was digitized by a computer system located in an adjoining room.

Behavioral Training. Rats were submitted to three phases of training: fear conditioning, extinction, and retrieval testing. For fear conditioning, rats were placed in the conditioning chambers in context A. The rats received five tone (10 s; 80 dB; 2 kHz)–footshock (1 s; 1 mA) trials [70-s intertrial interval (ITI)] beginning 3 min after being placed in the chambers. Sixty seconds after the final shock, the rats were returned to their home cages. Twenty-four hours after the conditioning session, rats were extinguished to the tone in a novel context (context B). On the extinction day, each rat spent 37 min in both context A and context B. In the extinction context, rats received 30 tone CS presentations (10 s; 80 dB; 2 kHz; 70-s ITI) 2 min after placement in the context, whereas in the context A, rats received no tone presentations. The retrieval testing phase took place 5 d after the extinction session either within the extinction context (context B, LOW FEAR) or outside the extinction context (context A, HIGH FEAR). Testing consisted of two 10-s tone CS presentations (80 dB; 2 kHz; 60-s ITI) beginning 2 min after placement in the context. Because fear conditioning in PSD-95:Venus transgenic rats has not been previously assessed, the first group of rats was designed as a behavioral control. These rats were trained according to the behavioral scheme described above and then each rat was tested for the fear memory retrieval twice: within the extinction context (context B, LOW FEAR) and outside the extinction context (context A, HIGH FEAR). The order of contexts in which the rats were tested was counterbalanced; the retrieval sessions took place on subsequent days. In addition, a control group that was exposed to the auditory stimuli but was not conditioned (NO-COND group) was included. The rats injected with anterograde tracers were tested only once, either inside or outside the extinction context. Fear to the tone CS during the training, extinction, and testing phases was assessed by measuring freezing behavior.

Immunohistochemistry. Two hours after the last behavioral session (retrieval testing), rats were overdosed with pentobarbital and transcardially perfused with ice-cold 0.1 M PBS (pH 7.4) and 4% (wt/vol) paraformaldehyde in PBS (pH 7.4). The brains were removed and stored in the same fixative for 24 h at 4 °C, and subsequently immersed in 30% (wt/vol) sucrose at 4 °C. The brains were then slowly frozen and sectioned at 40 μm on a cryostat. Coronal brain sections containing the prefrontal cortex, amygdala, and hippocampus were collected (32).

IF staining was performed on free-floating sections. The sections were washed with PBS with 0.2% Triton X-100 (PBST), blocked with 5% (vol/vol) normal donkey serum in PBST and incubated overnight at 4 °C with anti-GFP rabbit antibody (Invitrogen), diluted with 1% normal donkey serum (NDS) in PBST. The next day, sections were rinsed with PBST, before 1-h incubation at room temperature with a secondary antibody conjugated to Alexa Fluor 488 (1:500; Invitrogen). After several washes, the sections were mounted onto glass slides, air-dried, overlaid with the Vectashield Mounting Medium and covered with a glass coverslip. Alternatively, sections were washed three times in PBST. Endogenous peroxidases were quenched using a 0.3% solution of hydrogen peroxide in PBS (10 min). Following two more washes in PBST, sections were incubated overnight at 4 °C with an anti-GFP antibody (Millipore; AB3080; 1:250) diluted in PBST containing 4% (vol/vol) normal goat serum. The next day, sections were rinsed in PBST before incubation with a biotinylated goat anti-rabbit antibody (Vector Labs; 1:500). Following three washes, they were incubated with Vectastain ELITE ABC kit (1:500) in PBS for 1 h. After several rinses, staining was visualized using SigmaFast DAB kit. Sections were then washed, transferred to microscope slides, and dried

overnight. After brief washes in xylene (2 × 30 s), sections were mounted using Entellan mounting medium (Merck).

For double IF, the free-floating sections were washed with PBST, incubated (15 min) with antigen retrieval buffer (10 mM sodium citrate, 0.05% Tween 20, pH 6.0) in 90 °C, and then blocked with 5% (vol/vol) NDS in PBST. Then sections were incubated (4 °C overnight) with anti-GFP rabbit antibody combined with either anti-synaptophysin mouse antibody (Millipore) or c-Fos (Santa Cruz Biotechnology), diluted in 1% donkey normal serum in PBST. The sections were then rinsed in PBST and incubated at room temperature with the respective secondary antibodies conjugated to Alexa Fluor 488 (for anti-GFP labeling; 1:500) or Alexa Fluor 405 (1:500; Invitrogen). Alternatively, for double c-Fos/GFP immunolabeling sections were washed three times in PBS and incubated for 48 h at 4 °C with a rabbit anti c-Fos antibody (Santa Cruz; sc-52; 1:500) diluted in PBS containing 4% (vol/vol) NDS. Subsequently, the sections were washed in PBS with 0.3% Triton X-100 (PBST) and incubated with a secondary donkey anti-rabbit antibody conjugated to Alexa Fluor 555 (1:250; Life Technologies) for 2 h. Following several rinses in PBST, sections were incubated overnight with a rabbit anti-GFP antibody (Millipore; AB3080; 1:250) diluted in PBST containing 4% (vol/vol) NDS. The next day, sections were washed in PBST before an incubation with a secondary donkey anti-rabbit antibody conjugated to Alexa Fluor 488 (1:250; Life Technologies). Following three washes in PBS, sections were transferred to glass slides and mounted using Vectashield.

Image Capture and Analysis. The triple-labeling results were analyzed with the aid of confocal laser-scanning microscopy. The confocal system consisted of a Zeiss LSM5 Exciter microscope equipped with an Ar laser producing light at 467 and 488 nm, a Kr laser for 568 nm, and a HeNe laser for 647 nm light. Two objectives (20× and 63×) were used to scan the samples. A series of continuous optical sections, at 1-μm intervals along the z-axis of the tissue section, were scanned for all three fluorescent signals. The signal obtained for each fluorophore on one series of optical sections was stored separately as a series of 1,024 × 1,024 pixel images. The images were then processed with Imaris 6.3.1 software (Bitplane). PHA-L- and FR-labeled images were separately combined with Venus-stained cell bodies and proximal dendrites to analyze for the presence of close appositions between PHA-L- or FR-stained terminals and Venus-positive neurons in the ventral part of the La and the lateral part of the Ce.

Afferent terminals on Venus-positive neurons were analyzed in two scan images taken unilaterally for the vHIPP/PFC-injected rats and bilaterally for the IL/PL-injected rats under 20× objective within the ventral part of the La (−3.0 to −3.36 mm from bregma) and the lateral and capsular part of the Ce (−2.16 to −2.64 mm from bregma) (32). The potential contacts between PHA-L- and FR-labeled fibers and the Venus-positive neurons were estimated as numbers of voxels for axonal varicosities located in the close proximity to Venus-positive neurons. Then, the ratios of vHIPP/PFC and IL/PL projections (measured in voxels) were calculated for all Venus-positive neurons in a single scan image for the La and Ce and averaged between two images for each rat. In another analysis, the ratios of vHIPP/PFC and IL/PL projections were calculated for single Venus-positive neurons within the La. Moreover, the overall projections from the vHIPP and PFC, as well as IL and PL to the La were analyzed for the same images as projections to the activated neurons. The ratio of vHIPP/PFC and IL/PL projections (measured in voxels) was then calculated.

Statistical Analyses. For each conditioning session, the freezing data were transformed to a percentage of observations and analyzed with a repeated-measures analysis of variance (ANOVA). The group differences for the vHIPP/PFC and IL/PL projections ratios were analyzed using independent one-way ANOVAs for each brain structure. The Kolmogorov–Smirnov two-sample test was performed to compare differences between the rate of afferent projections from the vHIPP and PFC, as well as from the IL and PL onto the activated neurons in the LOW FEAR and HIGH FEAR groups. For each group, the cumulative frequency distributions of vHIPP/PFC and IL/PL projection ratios were made, and for each distribution the same eight intervals (0.0–0.5, 0.5–1.0, 1.0–1.5, 1.5–2.0, 2.0–2.5, 2.5–3.0, 3.0–3.5, and >3.5) were used. Sample sizes for vHIPP/PFC projection ratios were 160 active neurons in the LOW FEAR and 195 neurons in the HIGH FEAR groups. The respective sample sizes for the IL/PL projection ratios were 140 and 175 neurons. The test focused on the largest of the observed deviations. The data are represented as mean ± SEM unless it is marked otherwise.

1. Bouton ME, Westbrook RF, Corcoran KA, Maren S (2006) Contextual and temporal modulation of extinction: Behavioral and biological mechanisms. *Biol Psychiatry* 60: 352–360.
2. Maren S (2011) Seeking a spotless mind: Extinction, deconsolidation, and erasure of fear memory. *Neuron* 70:830–845.
3. Bouton ME, Bolles RC (1979) Role of conditioned contextual stimuli in reinstatement of extinguished fear. *J Exp Psychol Anim Behav Process* 5:368–378.
4. Boschen MJ, Neumann DL, Waters AM (2009) Relapse of successfully treated anxiety and fear: Theoretical issues and recommendations for clinical practice. *Aust N Z J Psychiatry* 43:89–100.
5. Falls WA, Miserendino MJ, Davis M (1992) Extinction of fear-potentiated startle: Blockade by infusion of an NMDA antagonist into the amygdala. *J Neurosci* 12:854–863.
6. Quirk GJ, Russo GK, Barron JL, Lebron K (2000) The role of ventromedial prefrontal cortex in the recovery of extinguished fear. *J Neurosci* 20:6225–6231.
7. Milad MR, Quirk GJ (2002) Neurons in medial prefrontal cortex signal memory for fear extinction. *Nature* 420:70–74.
8. Santini E, Ge H, Ren K, Peña de Ortiz S, Quirk GJ (2004) Consolidation of fear extinction requires protein synthesis in the medial prefrontal cortex. *J Neurosci* 24:5704–5710.
9. Vidal-Gonzalez I, Vidal-Gonzalez B, Rauch SL, Quirk GJ (2006) Microstimulation reveals opposing influences of prelimbic and infralimbic cortex on the expression of conditioned fear. *Learn Mem* 13:728–733.
10. Burgos-Robles A, Vidal-Gonzalez I, Quirk GJ (2009) Sustained conditioned responses in prelimbic prefrontal neurons are correlated with fear expression and extinction failure. *J Neurosci* 29:8474–8482.
11. Sierra-Mercado D, Padilla-Coreano N, Quirk GJ (2011) Dissociable roles of prelimbic and infralimbic cortices, ventral hippocampus, and basolateral amygdala in the expression and extinction of conditioned fear. *Neuropsychopharmacology* 36:529–538.
12. Orsini CA, Kim JH, Knapska E, Maren S (2011) Hippocampal and prefrontal projections to the basal amygdala mediate contextual regulation of fear after extinction. *J Neurosci* 31:17269–17277.
13. Herry C, et al. (2008) Switching on and off fear by distinct neuronal circuits. *Nature* 454:600–606.
14. Wilson Y, et al. (2002) Visualization of functionally activated circuitry in the brain. *Proc Natl Acad Sci USA* 99:3252–3257.
15. Pitkänen A, Pikkarainen M, Nurminen N, Ylinen A (2000) Reciprocal connections between the amygdala and the hippocampal formation, perirhinal cortex, and postrhinal cortex in rat. A review. *Ann N Y Acad Sci* 911:369–391.
16. Knapska E, Radwanska K, Werka T, Kaczmarek L (2007) Functional internal complexity of amygdala: Focus on gene activity mapping after behavioral training and drugs of abuse. *Physiol Rev* 87:1113–1173.
17. Robertson LM, et al. (1995) Regulation of c-fos expression in transgenic mice requires multiple interdependent transcription control elements. *Neuron* 14:241–252.
18. Barth AL, Gerkin RC, Dean KL (2004) Alteration of neuronal firing properties after in vivo experience in a FosGFP transgenic mouse. *J Neurosci* 24:6466–6475.
19. Matsuo N, Reijmers L, Mayford M (2008) Spine-type-specific recruitment of newly synthesized AMPA receptors with learning. *Science* 319:1104–1107.
20. Gilmartin MR, McEchron MD (2005) Single neurons in the medial prefrontal cortex of the rat exhibit tonic and phasic coding during trace fear conditioning. *Behav Neurosci* 119:1496–1510.
21. Knapska E, Maren S (2009) Reciprocal patterns of c-Fos expression in the medial prefrontal cortex and amygdala after extinction and renewal of conditioned fear. *Learn Mem* 16:486–493.
22. Corcoran KA, Maren S (2001) Hippocampal inactivation disrupts contextual retrieval of fear memory after extinction. *J Neurosci* 21:1720–1726.
23. Corcoran KA, Maren S (2004) Factors regulating the effects of hippocampal inactivation on renewal of conditional fear after extinction. *Learn Mem* 11:598–603.
24. Corcoran KA, Desmond TJ, Frey KA, Maren S (2005) Hippocampal inactivation disrupts the acquisition and contextual encoding of fear extinction. *J Neurosci* 25:8978–8987.
25. Ji J, Maren S (2005) Electrolytic lesions of the dorsal hippocampus disrupt renewal of conditional fear after extinction. *Learn Mem* 12:270–276.
26. Ji J, Maren S (2008) Differential roles for hippocampal areas CA1 and CA3 in the contextual encoding and retrieval of extinguished fear. *Learn Mem* 15:244–251.
27. Hobin JA, Ji J, Maren S (2006) Ventral hippocampal muscimol disrupts context-specific fear memory retrieval after extinction in rats. *Hippocampus* 16:174–182.
28. Vertes RP (2006) Interactions among the medial prefrontal cortex, hippocampus and midline thalamus in emotional and cognitive processing in the rat. *Neuroscience* 142:1–20.
29. Arnold DB, Clapham DE (1999) Molecular determinants for subcellular localization of PSD-95 with an interacting K⁺ channel. *Neuron* 23:149–157.
30. Wang KH, et al. (2006) In vivo two-photon imaging reveals a role of arc in enhancing orientation specificity in visual cortex. *Cell* 126:389–402.
31. Wilczynski GM, et al. (2008) Important role of matrix metalloproteinase 9 in epileptogenesis. *J Cell Biol* 180:1021–1035.
32. Paxinos G, Watson C (2007) *The Rat Brain in Stereotaxic Coordinates* (Academic, San Diego).